DOI: https://doi.org/10.24425/amm.2025.152570

S. KAZHIKENOVA[1*], G. SHAIKHOVA[1], S. SHALTAKOV[1]

INFLUENCE OF TEMPERATURE ON ULTRASOUND ABSORPTION AND STRUCTURAL PROPERTIES OF MELTS

Ultrasonic melt processing attracts considerable interest from both academic and industrial communities as a promising route improving melt quality. The significance of this problem is predetermined by the matter liquid state problem. In paper the ultrasound absorption and propagation speed v_S temperature are measured using multiple groups of samples, each group heated to a different temperature. This paper summaries the results on the evaluation of ultrasound absorption and the propagation speed, for calculating the ultrasound propagation speed in solutions, studies of the nucleation, growth and fragmentation of particles in liquid melts. It has been proven that melts with semiconductor properties are micro-inhomogeneous due to the existence of clusters in their atomic matrix. These results provide valuable new insights and knowledge that are essential for upscaling ultrasonic melt processing to industrial level.

Keywords: Ultrasound absorption; micro inhomogeneous melts; atomic mass; ultrasound propagation speed; coordination number

1. Introduction

The application of power ultrasound during liquid to solid transformation is believed to be an effective way to improve the solidification microstructures and mechanical properties [1]. In fact, the entire arsenal of modern experimental and theoretical physics is connected to the research of the physicochemical behavior of melts [2]. Acoustic methods are the most promising among experimental methods for research of the matter liquid state. They are simple, reliable, highly sensitive to changes of matter structure and the interatomic interaction.

The results of this research make it possible to predict the melts elastic properties of simple substances and extend it to complex substances.

At present, the electrophysical, thermophysical, thermodynamic and viscous properties of liquid semimetals and semiconductors based on the electronics industry have been widely studied.

However, the ongoing research in the field of studying these properties is not sufficient to solve the problem of the liquid semimetals and semiconductors structure. It is also impossible to obtain an unambiguous result by only structural research. In this aspect, it is known that «modern acoustic research methods are a powerful tool for obtaining information about the structure of melts and semiconductors» [3]. Melts and semiconductors were not widely also studied, since the high-temperature acoustic experiments technology with aggressive melts of semimetals and semiconductors complicated the research process [1-5]. Our research includes: development liquid semimetals and semiconductors structure model; experimental and theoretical studies of the propagation speed and absorption coefficient of ultrasound temperature dependences in liquid semimetals and semiconductors; regularities generalization of liquid metals, semimetals and semiconductors structural properties.

A hypothesis about the micro-inhomogeneous structure of liquids arose in connection with Stuart's research using X-rays in the 1920. Micro-inhomogeneity extends to any melts from alkali metals to semiconductors. But the hypothesis remained a hypothesis, since there were no interpreted experimental data. The experiments were performed with a solidification apparatus incorporated with ultrasonic generator. The propagation of elastic waves is associated with the fundamental properties of material media, including the mass of particles, their space, the bonds between particles of matter. These indicators, namely, the inertial factor (mass of particles), the spatial factor (volume per particle), the stiffness factor between particles (compressibility), are sufficient fora general description of elastic waves absorption and propagation speed [6].

[1] SAGINOV TECHNICAL UNIVERSITY, KARAGANDA, KAZAKHSTAN

* Corresponding author: sauleshka555@mail.kz

2. Main results

As is known, the absorption coefficient is determined by the Stokes-Kirchhoff formula in the general case [7]:

$$\beta = \frac{2\pi^2 f^2}{\rho v_s^3}\frac{4}{3}\eta + \chi\left(\frac{1}{C_V} - \frac{1}{C_P}\right)$$

χ is the thermal conductivity coefficient, C_V, C_P is the heat capacity at constant volume, pressure.

The Stokes-Kirchhoff formula will take the form after the replacement $\gamma = \frac{C_P}{C_V}$:

$$\beta = \frac{2\pi^2 f^2}{\rho v_S^3}\left[\frac{4}{3}\eta + \frac{\chi}{C_P}(\gamma - 1)\right] \quad (1)$$

We will transform formula (1) to inertial, coupling and spatial factors based on the parameters $\eta = \rho\upsilon$, υ is the kinematic viscosity, $\frac{1}{\rho v_S^2} = \alpha_S$ is the adiabatic compressibility, $C_P = \frac{dQ}{dT}\frac{1}{m}$ is the melt heat capacity:

$$\frac{\beta v_S}{f^2} = 2\pi^2\alpha_S\left[\frac{4}{3}\rho\upsilon + \frac{\chi}{\left(\frac{dQ}{dT}\right)_P}m(\gamma - 1)\right] \quad (2)$$

Let $\rho = \frac{m}{V} = \frac{N_A M_A}{N_A V_A}$ and $m = N_A M_A$, N_A is the Avogadro number, M_A is the atomic mass, V_A is the atomic volume,

$$\sigma = 2\pi^2\alpha_S\left[\frac{4}{3}\frac{\upsilon}{V_A} + \frac{\chi}{\left(\frac{dQ}{dT}\right)_P}N_A(\gamma - 1)\right]$$

Then we rewrite equality (2) in the form:

$$\frac{\beta v_S}{f^2} = \sigma M_A \quad (3)$$

The obtained Eq. (3) makes acoustic parameters monitoring in simple substances melts more accessible. Experimental measurements monitoring by value using reference data [8-12] is shown in Fig. 1. We have established the correlation dependence between measurement results $\frac{\beta v_S}{f^2}$ and the parameter values M_A, where σ is a constant value for each group. Note: the bonding factors intragroup similarity not only observed in condensed bodies, but also diatomic molecules it.

The highest value of the dissociation energy is observed for five electrons in the outer shell, the most rigid bonds exist in diatomic molecules [13]. Local bonds become stronger (partial atomic association) with an increase in the number of external electrons in melts due to the electron redistribution. There is no redistribution of electrons in diatomic molecules, since they bond

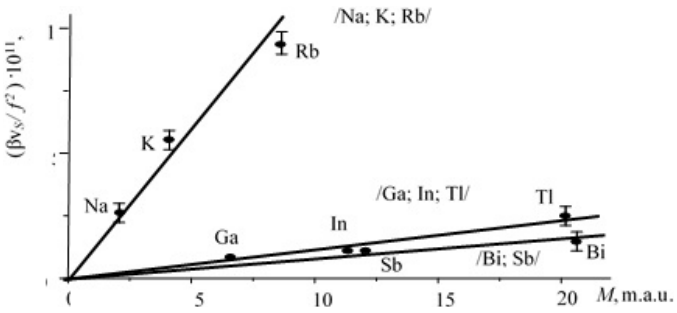

Fig. 1. $\frac{\beta v_S}{f^2}$ – M simple substances dependence at crystallization temperatures

with a single direction from one atom to another. If the number of external electrons is more than five in diatomic molecules, then individual electrons are transformed into a non-bonding state. This situation is explained by a decrease in the dissociation energy of diatomic molecules, starting from the oxygen group [13]. The closest packing coordination number (the number of bonds realization directions) can reach twelve in condensed matter. If there are more electrons than necessary to implement a uniform bond, they are redistributed. As a result, bonds more rigid are formed between individual neighboring atoms, associations of atoms are created.

It should be noted that the weakening of bonds between associates leads to an increase in bonds in associates and a decrease in the overall rigidity of the melt macroscopic volume. This is confirmed by the sulfur group example. There is a high correlation between the parameter $\frac{\beta v_S}{f^2}$ and the atom associates in the liquids of this group. The experimental values will be equal

$$\frac{\beta v_S}{f^2} = 19\times10^{-11}\text{ c for } S, \quad \frac{\beta v_S}{f^2} = 6{,}7\times10^{-11}\text{ c for } Se,$$

$$\frac{\beta v_S}{f^2} = 1{,}34\times10^{-11}\text{ c for } Te,$$

which indicates a decrease the atom associates in *S*, *Se*, *Te* melts.

We have shown in Fig. 1 that the parameter $\frac{\beta v_S}{f^2}$ increases from *Na* to *Rb* in the alkali metal series. This is confirmed by the fact that these groups of metals are prone to structure loosening with increasing atomic mass M_A. The $\frac{\beta}{f^2}$ temperature dependence is quite complex. Immediately after melting, there is a decrease in the absorption coefficient of ultrasonic waves, which increases monotonically with increasing temperature. This includes the alkali metals and further all other simple metals that are densely packed in the solid state.

Two-component liquid-metal solutions with monotonically increasing ultrasound absorption polytherms should also be attributed to this class. The absorption coefficient of ultrasonic waves decreases immediately after melting. In addition, the absorption coefficient of ultrasonic waves increases monotonically with increasing temperature. This includes the alkali metals

and further all other simple metals that are densely packed in the solid state. Melts, in which the absorption polytherms of ultrasonic waves do not increase monotonically with temperature, belong to the second class. This class includes semimetals and semiconductors, in which significant structural changes occur during melting. All melts with anomalous behavior of absorption polytherms and propagation rates (bismuth, antimony, tellurium, etc.) are characterized by the fact that their structural changes continue in a certain temperature range after melting.

This is especially pronounced in tellurium, antimony melts, etc. The polytherm $\frac{\beta}{f^2}$ anomalous behavior temperature interval of these melts coincides with the «after-melting» temperature interval. The experimental results on Eq. (3) are also can be used for compounds. For monitoring, let us consider GaSb and InSb compounds. Methods of descriptive statistics were used to systematize and describe the data. Experimental measurements monitoring by value using reference data [8-12] is shown in Fig. 1. The experimental results are shown in Figs. 2-12 for GaSb and InSb, $Bi_{0,25}Sb_{0,75}$, $Bi_{0,5}Sb_{0,5}$, $Bi_{0,75}Sb_{0,25}$, Bi-Sb, $Sn_{0,30}Te_{0,70}$, $Sn_{0,5}Te_{0,5}$, $Sn_{0,70}Te_{0,30}$, Sn-Te compounds. We used the TABLE 1 and TABLE 2 experimental measurements to build Figure with markers in Excel. The solid lines are the result of the experimental data approximation by the equation

$$v_S(T) = v_{SL} - \beta(T - T_L)$$

$\beta = \frac{dv_S}{dT}$ is the ultrasound propagation speed temperature coefficient, T_L is melting point, v_{SL} is ultrasound propagation speed at T_L.

Dependence $\beta = \frac{dv_S}{dT}$ – M is shown in Fig. 2 for these compounds.

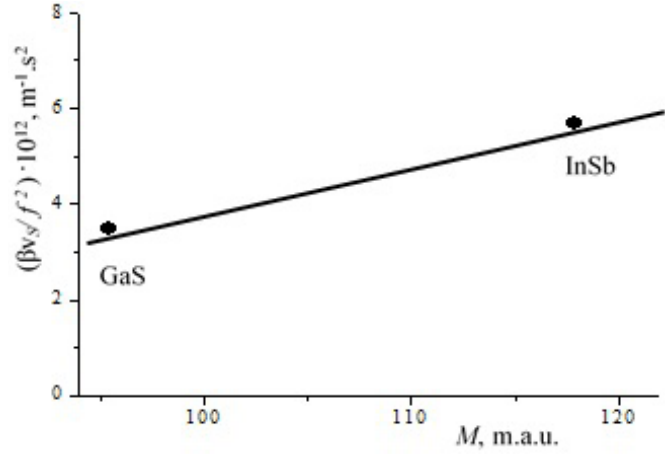

Fig. 2. Dependence $\frac{\beta v_S}{f^2}$ – M for GaSb and InSb systems

Thus, the acoustic analysis in electron melts experimental measurements shows that the absorption polytherms and the propagation velocity behavior of ultrasonic waves depends on the semimetals and semiconductors acoustic properties. This was the reason for separating these melts into an electron melts separate class. A straight-line relationship between $\frac{\beta v_S}{f^2}$ and M_A inertial factor has been established.

For calculations, melt compounds were rotated by acoustically equivalent liquids from atoms of the same type by mass that satisfies the condition

$$M = M_1 X_1 + M_2 X_2 \quad (4)$$

M_1, M_2 – atoms mass; X_1, X_2 – components atomic fractions.

The experimental results on Eq. (3) are also can be used for compounds. Let us consider Bi-Sb compound. The experimental results are shown in Figs. 3-5 for $Bi_{0,25}Sb_{0,75}$, $Bi_{0,5}Sb_{0,5}$, $Bi_{0,75}Sb_{0,25}$ compounds.

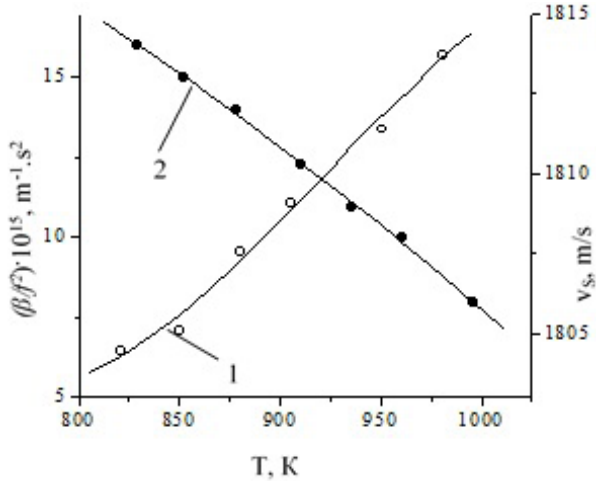

$1 - \frac{\beta}{f^2}$, $2 - v_S$

Fig. 3. Temperature dependence of ultrasonic absorption coefficient and propagation speed in the Bi-Sb system (composition $Bi_{0,25}Sb_{0,75}$)

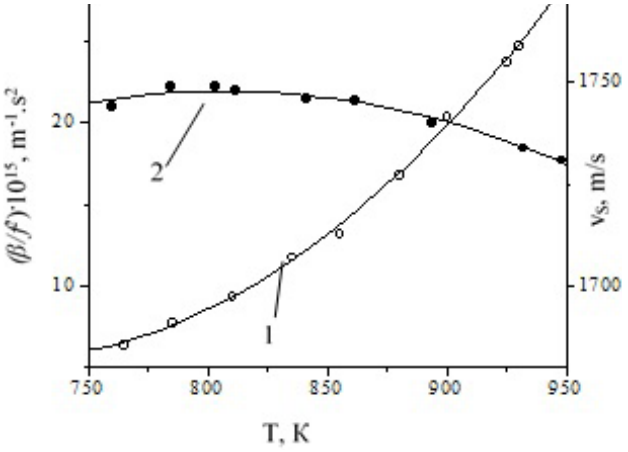

$1 - \frac{\beta}{f^2}$, $2 - v_S$

Fig. 4. Temperature dependence of ultrasonic absorption coefficient and propagation speed in the Bi-Sb system (composition $Bi_{0,5}Sb_{0,5}$)

We have found that the ultrasound absorption coefficient increases with temperature in all Bi-Sb compositions. Dependence

TABLE 1

Temperature dependence of Ultrasound absorption

Ga		Bi		Sb		Ge		Se		Te	
T, К	$\frac{\beta}{f^2}\times10^{15}$	T, К	$\frac{\beta}{f^2}\times10^{15}$	T, К	$\frac{\beta}{f^2}\times10^{15}$	T, К	$\frac{\beta}{f^2}\times10^{15}$	T, К	$\frac{\beta}{f^2}\times10^{15}$	T, К	$\frac{\beta}{f^2}\times10^{15}$
302	2,2	526	9,2	902	5,45	1211	1,56	520	725	734	14,5
325	2,9	545	9,3	918	5,28	1213	1,53	526	635	750	14,2
335	3,3	565	9,5	945	5,2	1220	1,5	544	630	762	13,8
370	3,5	599	9,8	960	5,44	1226	1,59	560	665	730	13,2
395	3,1	610	9,9	970	5,6	1229	1,6	574	565	812	13
405	3,4	615	10	986	5,8	1239	1,5	620	610	830	12,9
425	2,8	630	10,3	1000	5,83	1247	1,49	624	680	862	13
450	2	635	10,7	1020	6,4	1254	1,46	652	735	883	13,1
475	1,4	660	10,8	1035	6,5	1262	1,45	682	825	902	13,2
500	1,2	710	11,1	1050	7	1267	1,51	702	815	912	13,3
520	1,2	730	11,3	1078	7,3	1271	1,68	**InTe**		992	13,5
545	1,22	735	11,7	1094	7,5	1277	2,1	980	19,6	974	14,1
575	1,18	740	12	1104	7,8	1283	2,62	990	19,01	1006	15,1
585	1,28	755	12,4	1129	8,2	**Ga_2Te_3**		948	18,5	1051	17
595	1,3	770	12,9	1138	8,9	1065	110,1	1010	18	1078	17,5
615	1,6	775	13,2	**GaTe**		1075	94,01	1025	17,5	1098	18,1
685	2,8	805	13,6	1100	62,1	1085	84,1	1040	16,9	1106	18,9
705	3,2	815	14,9	1112	56,2	1097	65,1	1050	16,6	**In_2Te_3**	
745	3,6	820	15,4	1125	50,5	1110	55,2	1060	16,4	965	75,01
GaSb		835	15,9	1141	45,1	1112	50	1070	16,2	975	56,02
985	1,6	840	16,8	1167	38,1	1130	45,2	1085	15,8	905	42
1000	1,3	849	16,9	1178	35,8	1148	40,1	1097	15,5	1000	34
1020	1,2	855	17,3	1194	33,1	1160	38	**Bi_2Te_3**		1015	26,2
1040	1,5	875	17,7	1204	28	1185	37	862	30	1030	22,1
1055	2,3	900	18,2	1228	24,2	1200	35,5	875	29,4	1040	21
1070	3	905	18,5	**InSb**		**Sb_2Te_3**		890	29	1055	20,3
1077	3,8	910	19	814	2,78	902	24,4	900	28,5	1070	17
1090	4,4	915	19,5	820	2,65	909	23,1	930	27,4	1095	15,2
1105	5,4	935	20,8	840	2,9	923	22	956	26,5	**$Bi_{0,5}Sb_{0,5}$**	
1115	6,38	**Sb_2Se_3**		855	3,1	933	21	978	25,8	765	6,4
Bi_2Se_3		890	35,1	870	3,7	948	18,5	1009	25	785	7,8
1000	33	903	31,9	880	3,8	969	16,5	1042	24	810	9,4
1005	32,01	905	30	895	4,38	983	15	1080	23,4	835	11,8
1018	30,7	907	28	905	4,9	1007	14,1	**$Bi_{0,25}Sb_{0,75}$**		855	13,2
1025	30	912	27	920	5,4	1030	13,8	821	6,5	880	16,8
1037	29,3	915	25	930	5,98	1049	14	850	7,1	900	20,4
1045	28,8	928	22,6	935	6,2	1064	14,3	880	9,6	925	23,8
1049	28,7	935	20,8	950	6,6	1073	15	905	11,1	930	24,8
1060	28	940	20	969	7,3	**$Sn_{0,7}Te_{0,3}$**		950	13,4	**In**	
1070	27,8	955	21,5	**SnTe**		984	11,4	980	15,7	440	4,3
1074	27,7	965	19	1069	22,8	995	11,7	**Sn**		462	4,4
1090	27,5	975	18,9	1092	23,3	1020	12	500	4,8	500	4,8
1095	27,4	1000	18,1	1110	23,5	1045	12,2	560	5,4	520	5
$Bi_{0,75}Sb_{0,25}$		1019	18	1123	24	1050	12,7	584	5,1	570	5,9
670	7,5	**$Sn_{0,3}Te_{0,7}$**		1132	23,8	1080	14	619	5	598	6,9
690	9,5	868	18,5	1142	24,4	1087	14,5	680	6,5	625	7,3
710	12,8	890	18,4	1157	25,5	1111	16	740	9,5	640	7,8
730	17	910	19,5	1175	27,9	1116	17	820	10,5	675	8,6
745	19,8	938	20,6	1195	29			880	12	681	8,7
775	25,5	980	21					940	12,4	720	9,5
800	30,1	1020	23					980	12,6	740	10,2
670	7,5	1060	24,8					1000	13,4	770	11
		1080	26,8					1060	13,4		
								1120	15,2		

TABLE 2

Temperature dependence of Ultrasound propagation speed

Ga		**Bi**		**Sb**		**Se**		**Te**		**GaTe**	
***T*, К**	v_s	***T*, К**	v_s	***T*, К**	v_s	***T*, К**	v_s	***T*, К**	v_s	***T*, К**	v_s
304	2866	527	1640	915	1902	501	1087	730	935	1101	1330
310	2868	546	1643	927	1911	514	1075	738	955	1109	1327
316	2870	549	1641	940	1915	526	1063	750	980	1131	1322
320	2865	565	1639	955	1914	546	1043	762	990	1150	1321
324	2860	585	1639	964	1913	564	1030	744	1015	1156	1319
328	2854	599	1638	970	1917	572	1018	786	1035	1174	1316
330	2853	601	1636	980	1920	584	1005	798	1045	1215	1315
335	2856	615	1636	990	1922	600	995	814	1050	**Ga_2Te_3**	
340	2858	660	1633	1000	1920	618	980	830	1060	1073	1156
345	2853	670	1630	1005	1919	644	960	851	1075	1082	1152
348	2847	672	1627	1020	1917	658	955	874	1090	1091	1151
355	2844	675	1621	1038	1914	668	945	898	1100	1105	1146
365	2848	730	1620	1054	1917	674	937	922	1110	1122	1142
370	2849	735	1619	1074	1917,5	682	925	938	1120	1144	1140
374	2841	755	1617	1090	1918	688	918	950	1125	1160	1141
378	2834	785	1613	**In_2Te_3**		**Sb_2Se_3**		905	970	1125	1174
389	2836	808	1607	955	1160	890	1124	990	1123	1200	1139
396	2838	850	1600	960	1155	900	1118	998	1135	**Sb_2Te_3**	
398	2837	900	1590	989	1151	907	1113	1018	1130	888	1225
406	2835	960	1587	1017	1150	922	1107	1038	1135	905	1230
412	2835	**InTe**		1057	1152	925	1106	1070	1140	913	1235
416	2835	984	1248	1071	1156	933	1102	1082	1135	921	1238
424	2832	992	1250	1082	1163	937	1097	Bi_2Se_3		924	1239
430	2832	1006	1054	1089	1666	946	1104	999	1398	938	1244
434	2830	1020	1056	**$Bi_{0,25}Sb_{0,75}$**		952	1103	1010	1395	946	1251
440	2827	1040	1060	829	1814	957	1103	1027	1390	951	1251,5
444	2819	1065	1072	852	1813	964	1099	1038	1385	961	1256
459	2823	1079	1077	878	1812	970	1097	1044	1368	970	1258
464	2823	**Bi_2Te_3**		840	910	974	1095	1060	1360	980	1259
475	2820	865	1397	935	1809	976	1093	1070	1358	983	1259
484	2816	876	1397	960	1808	980	1088	1074	1357	985	1259
506	2813	890	1396	995	1806	989	1081	1090	1350	994	1259
508	2809	900	1396	**$Bi_{0,5}Sb_{0,5}$**		995	1077	1095	1354	1006	1264
520	2804	905	1394	760	1744	1000	1078	**Sn**		1015	1267
539	2800	912	1393	784	1749	1009	1075	510	2478	1023	1270
562	2797	924	1391	803	1749	1019	1077	538	2472	1033	1272
600	2790	933	1388	811	1748	**SnTe**		559	2463	1044	1275
644	2778	942	1383	841	1746	1065	1533	578	2464	1060	1276
666	2768	952	1385	861	1745,5	1080	1531	600	2473	**In**	
692	2762	965	1387	894	1740	1090	1528	650	2450	470	2307
715	2756	998	1374	832	1734	1099	1526	682	2445	490	2301
740	2740	1009	1378	848	1731	1109	1522	800	2414	530	2295
$Sn_{0,30}Te_{0,70}$		1050	1370	**$Bi_{0,75}Sb_{0,25}$**		1127	1523	860	2404	550	2290
865	1452	1070	1369	668	1698	1137	1520	900	2385	590	2278
960	1449	1090	1368,5	700	1694	1146	1517	950	2380	660	2264
935	1446	**$Sn_{0,70}Te_{0,30}$**		718	1690	1161	1516	1000	2364	730	2250
960	1441	983	1929	750	1688	1182	1513	1050	2355	770	2242
982	1438	1005	1926	776	1687	1199	1510	1060	2350	820	2232
1025	1428	1025	1921	811	1684,5			1070	2348	850	2224
1040	1425	1047	1920	850	1679			1108	2335		
1050	1422	1070	1917								
1080	1417	1082	1912								
		1102	1908								
		1115	1905								

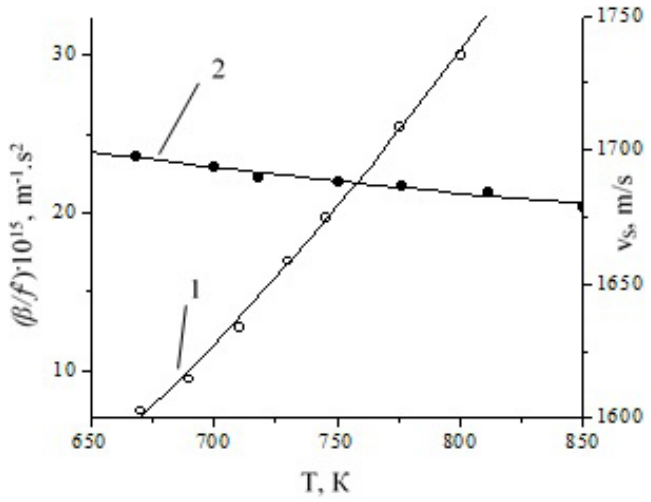

$1 - \frac{\beta}{f^2}$, $2 - v_S$

Fig. 5. Temperature dependence of ultrasonic absorption coefficient and propagation speed in the Bi-Sb system (composition $Bi_{0,75}Sb_{0,25}$)

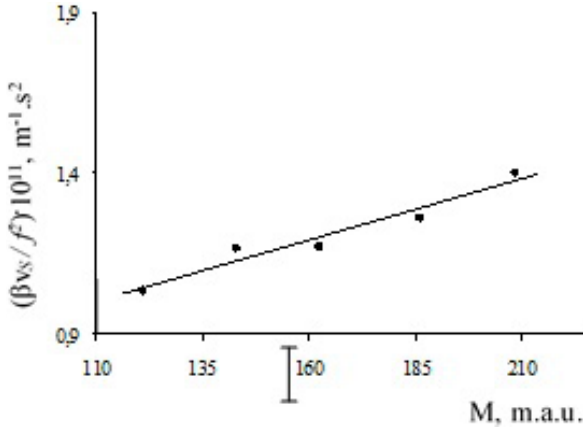

Fig. 6. Dependence $\frac{\beta v_S}{f^2} - M$ for Bi-Sb system

$\frac{\beta v_S}{f^2} - M_A$ is shown in Fig. 6 for these $Bi_{0,25}Sb_{0,75}$, $Bi_{0,5}Sb_{0,5}$, $Bi_{0,75}Sb_{0,25}$ compounds. We approximated the experimental data with a linear function during their processing, the graph of which is a straight line. The linear function coefficients were calculated using the least squares method. The experimental data are practically placed on straight lines in Fig. 6. This confirms the closeness of the calculated indicators to the ideal ones. Indeed, the authors of [14] showed that the Bi-Sb system forms a regular solutions series with atoms random arrangement. The results in the coordinates $\frac{\beta v_S}{f^2} - M_A$ are shown for the Sn-Pb system in Fig. 7. We found that the $\frac{\beta v_S}{f^2}$ experimental measurements are practically placed on straight lines according to Pless's experiment. Note that the indicated results are typical only for ideal systems, that is, for melts with an atoms random distribution. Ideal solutions are solutions in which a negligibly small interaction between the particles of the constituent substances is assumed.

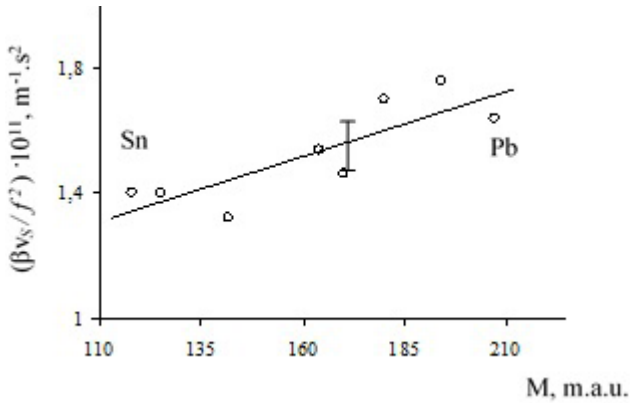

Fig. 7. Dependence $\frac{\beta v_S}{f^2} - M$ for Sn-Pb system [15]

We have developed an algorithm for determining the ideality or non-ideality degree of an arbitrary binary system based on monitoring the ultrasonic absorption coefficient and propagation speed experimental measurements. These are $v_S^2 - \frac{1}{M_A}$ and $\frac{\beta v_S}{f^2} - M_A$ diagrams.

We study the Sn-Te system, which forms a congruently melting semiconductor chemical SnTe compound. The ultrasound speed and absorption experimental measurements in the compositions $Sn_{0,30}Te_{0,70}$, $Sn_{0,5}Te_{0,5}$, $Sn_{0,70}Te_{0,30}$ are shown in Figs. 8-10. The ultrasound speed and absorption for liquid tin experimental measurements are shown graphically in Fig. 11.

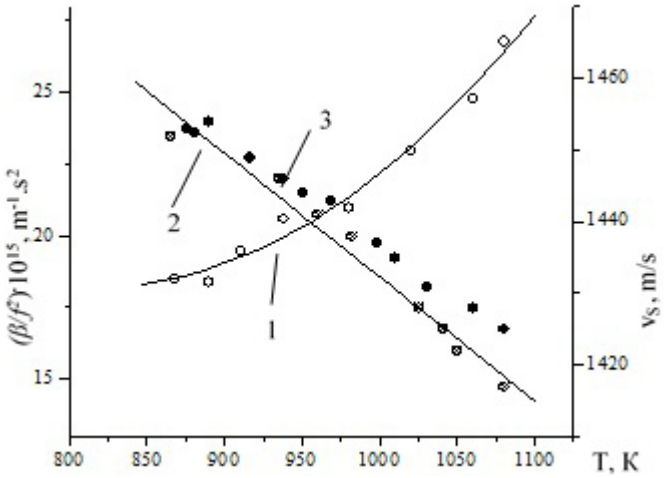

$1 - \frac{\beta}{f^2}$ the present work data, $2 - v_S$ the present work data, $3 - v_S$ [16] work data

Fig. 8. Temperature dependence of ultrasonic absorption coefficient and propagation speed in $Sn_{0,30}Te_{0,70}$ melts

We show a diagram for the Sn-Te system, it was previously studied by the [16,17] authors in Fig. 12. Calculations show that there are inconsistencies between the real isotherm and $\frac{\beta v_S}{f^2} - M_A$ linearity. Previously, for Bi-Sb and Pb-Sn systems,

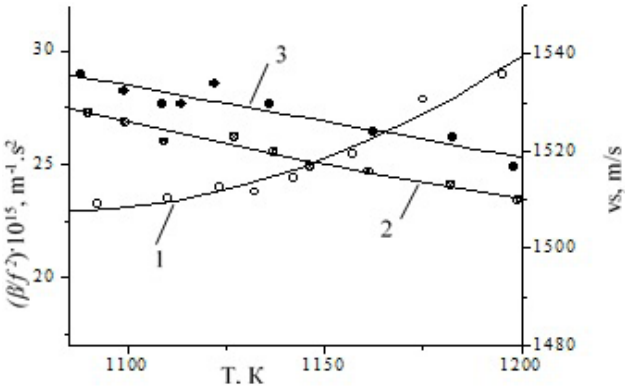

$1 - \frac{\beta}{f^2}$ the present work data, $2 - v_S$ the present work data,
$3 - v_S$ [16] work data

Fig. 9. Temperature dependence of ultrasonic absorption coefficient and propagation speed in $Sn_{0,5}Te_{0,5}$ melts

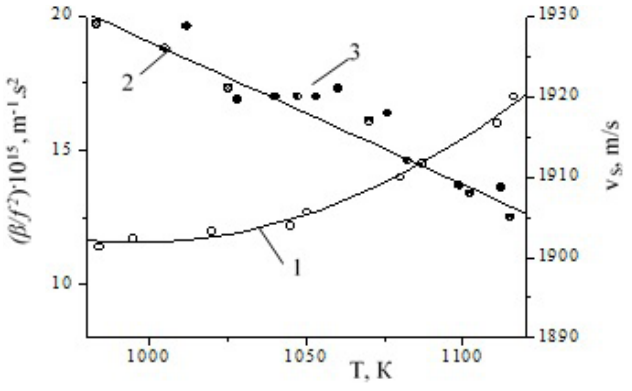

$1 - \frac{\beta}{f^2}$ the present work data, $2 - v_S$ the present work data,
$3 - v_S$ [16] work data

Fig. 10. Temperature dependence of ultrasonic absorption coefficient and propagation speed in $Sn_{0,70}Te_{0,30}$ melts

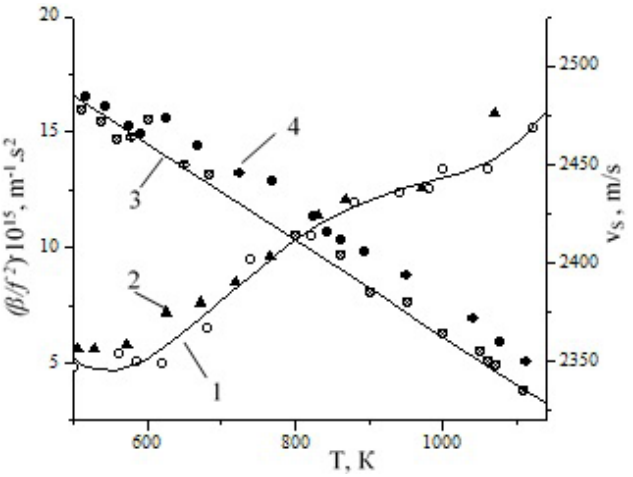

$1 - \frac{\beta}{f^2}$, $3 - v_S$ the present work data, $2 - \frac{\beta}{f^2}$ [16] work data,
$4 - v_S$ [16] work data

Fig. 11. Temperature dependence of ultrasonic absorption coefficient and propagation speed in liquid tin

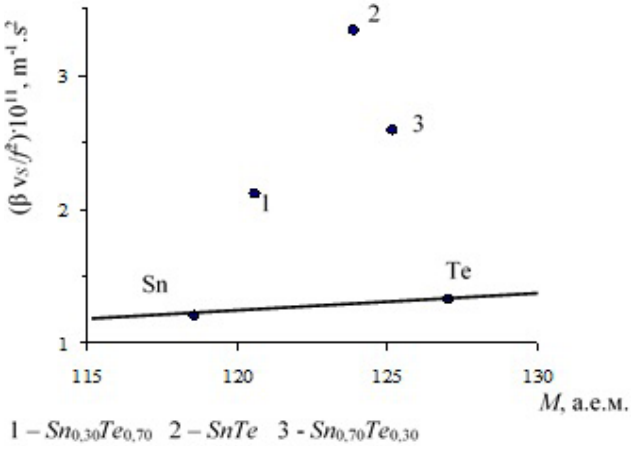

$1 - Sn_{0,30}Te_{0,70}$ $2 - SnTe$ $3 - Sn_{0,70}Te_{0,30}$

Fig. 12. Dependence $\frac{\beta v_S}{f^2} - M$ for Sn-Te system

it was found that these deviations are associated with melts microheterogeneity of intermediate concentrations. We have obtained a connection between the real isotherm $\frac{\beta v_S}{f^2} = f(M_A)$ and the corresponding linear diagram, which will allow us to evaluate the homogeneity or inhomogeneity of the melts and solutions. Consider a melt of the SnTe compound stoichiometric composition. We calculate the SnTe experimental measurement $\frac{\beta v_S}{f^2}$ and represent in Fig. 12 with the number 2. Through this point we draw a straight line parallel to the M axis. Let us assume that the SnTe melt is atomic and calculate the average M_A atomic mass by formula (4). An atomic SnTe melt corresponds to an extremely large M_A mass in an idealized system characterized by a linear dependence $\frac{\beta v_S}{f^2} - M_A$. As a result, the atomic mass of a real melt largely exceeds the average value atomic mass of the components. This unambiguously takes place in a situation where a real *SnTe* melt consists not only atoms of tin and tellurium, but also larger particles, such as clusters or associates, whose masses exceed the component atoms masses.

To quantify statistical errors in the measurements we used simple descriptive statistics. The statistical error of a purely random sample is estimated by the formula:

$$\Delta = t\sqrt{\frac{\sigma^2}{n}}$$

Consider *Ga* as an example. The mean value is 2.272631579. The statistical or standard error is 0.215733269. The 95% confidence level is between 2 and 2.4. This means that if similar or random samples were re-selected, then about 95% of these samples would have average values between 2 and 2.4.

Ga			
Temperature		**Ultrasound absorption**	
Mean	502,7368421	Mean	2,272631579
standard error	30,41677766	standard error	0,215733269

Median	500	Median	2,2
Mode	#	Mode	2,8
Standard deviation	132,58366	Standard deviation	0,940359518
Sample variance	17578,4269	Sample variance	0,884276023
Kurtosis	–0,930109426	Kurtosis	–1,828842923
Skewness	0,217917553	Skewness	0,058423005
Rang	443	Rang	2,42
Minimum	302	Minimum	1,18
Maximum	745	Maximum	3,6
Sum	9552	Sum	43,18
Count	19	Count	19
Confidence level (95.0%)	63,90327858	Confidence level (95.0%)	0,45323878

We calculated statistical errors for all measurements from TABLE 3 and TABLE 4.

3. Conclusion

We used significance testing to compare results to determine if one is better than the other. Descriptive statistics were used using the parametric criterion (Student's t-test) to perform the analysis. Student's t-test can be used to determine if there are statistically significant differences between datasets.

Consider Ge as an example. Consider the results of the F-test to determine if there is a significant difference between the deviations. The results give three important values:

- F: ratio between dispersions.
- P (F <= *f*) one-tail: the probability that variable 1 does not actually have a larger variance than variable 2. If it is greater than $\alpha = 0.05$, then there is no significant difference between the variances.
- F Critical one- tail: the value of F required for P (F <= *f*) = α. If this value is greater than F, it also means that there is no significant difference between the deviations.

F-test Two-sample for variance		
	Variable 1	**Variable 2**
Mean	1,660769231	1,649230769
Variance	0,111474359	0,111024359
Observations	13	13
df	12	12
F	1,004053165	
P(F <= *f*) one-tail	0,497262556	
F critical one-tail	2,686637112	

In our case P = 0.497263 > α = 0.05, also Fcr. = 2.686637 > F = 1.004053. Therefore, there is no significant difference between the deviations.

We choose the appropriate T-test. As in the F-test, if P (T <= *t*) is greater than $\alpha = 0.05$, then there is no significant difference. However, in this case, two P values are given: one for the single-tailed test and the other for the double-tailed test. In this case, we use a double-tailed value, since any variable that has a larger mean will be a significant difference.

T-test: Two-sample assuming equal variances		
	Variable 1	**Variable 2**
Mean	1,660769231	1,649230769
Variance	0,111474359	0,111024359
Observations	13	13
Pooled variance	0,111249359	
Hypothesized mean	0	
df	24	

TABLE 3

Statistical errors of Temperature dependence of Ultrasound absorption

Compounds	Statistical errors	Compounds	Statistical errors	Compounds	Statistical errors
Ga	0,215733	**Bi**	0,670372	**Sb**	0,303635
Ge	0,092601	**Se**	27,1728	**Te**	0,482402
GaSb	0,582494	**GaTe**	4,298808	**Ga_2Te_3**	7,758811
InTe	0,408283	**In_2Te_3**	6,164237	**Bi_2Se_3**	0,532322
Sb_2Se_3	1,489689	**InSb**	0,440256	**Sb_2Te_3**	1,146368
Bi_2Te_3	0,735754	**In_2Te_3**	6,164237	**$Bi_{0,75}Sb_{0,25}$**	2,991442
$Sn_{0,3}Te_{0,7}$	1,076162	**SnTe**	0,720425	**$Sn_{0,7}Te_{0,3}$**	0,666458
Sn	1,060004	**In**	0,62987		

TABLE 4

Statistical errors of Temperature dependence of Ultrasound propagation speed

Compounds	Statistical errors	Compounds	Statistical errors	Compounds	Statistical errors
Ga	4,873843	**Bi**	3,83035	**Sb**	1,242948
Sn	13,03025	**Se**	14,37275	**Te**	14,21959
In	9,527796	**GaTe**	2,080031	**Ga_2Te_3**	3,708099
InTe	34,30029	**In_2Te_3**	63,85878	**Bi_2Se_3**	5,854248
Sb_2Se_3	3,144983	**SnTe**	2,224209	**Sb_2Te_3**	3,350349
$Bi_{0,25}Sb_{0,75}$	128,6236	**$Bi_{0,5}Sb_{0,5}$**	2,196026	**$Bi_{0,75}Sb_{0,25}$**	2,34702
$Sn_{0,3}Te_{0,7}$	4,236088	**$Sn_{0,7}Te_{0,3}$**	2,986577		

t-stat	0,088197409	
P(T <= *t*) one-tail	0,465225799	
t critical one-tail	1,71088208	
P(T <= *t*) two-tail	0,930451597	
t critical two-tail	2,063898562	

In our case P = 0.930452 > α = 0.05, also tcr. = 2.063899 > *t* = 0.088197. Therefore, our results are statistically significant.

This work demonstrated the feasibility and practical value of direct acoustic measurements in liquid metals. These measurements can be used for optimization of ultrasonic melt processing. The physical and chemical effects of ultrasound on liquid melts structure were investigated. In our study with specific components and ultrasound system, we determined that the chemical effect is an irreversible and permanent change in atom weight and the atom-weight distribution due to ultrasound. As the ultrasound intensity increases, the atom weight of liquid metals reduces and its atom-weight distribution becomes narrower; the orientation of liquid metals atom along the flow direction reduces (in melt state). Ultrasound vibration increases the motion of atom chains and makes them more disorder; it also affects the relaxation process of liquid metals, leading to weakening the elastic effect.

Acknowledgments

The research relevance is confirmed by the financial support of the MSHE Science Committee of the Kazakhstan Republic, project AP23486482.

REFERENCES

[1] R.K. Chinnam, C. Fauteux, J. Neuenschwander, J. Janczak-Rusch, Evolution of the microstructure of Sn–Ag–Cu solder joints exposed to ultrasonic waves during solidification. Acta Materialia **59**, 1474-1481 (2011). DOI: https://doi.org/10.1016/j.actamat.2010.11.011

[2] S.Sh. Kazhikenova, S.N. Shaltakov, B. Nussupbekov, Difference melt model, Archives of Control Sciences **31** (LXVII), 607-627 (2021). DOI: https://doi.org/10.24425/acs.2021.138694

[3] M. Mesaros, O.E. Martínez, G.M. Bilmes, J.O. Tocho, Acoustic detection of laser induced melting of metals. J. Appl. Phys. **81** (2), 1014 (1997). DOI: https://doi.org/10.1063/1.364196

[4] L. Hackett, M. Miller, S. Weatherred, Non-reciprocal acousto-electric microwave amplifiers with net gain and low noise in continuous operation. Nat Electron. **6**, 76-85 (2023). DOI: https://doi.org/10.1038/s41928-022-00908-6

[5] D.L. White, Amplification of ultrasonic waves in piezoelectric semiconductors. J. Appl. Phys. **33**547-2554 (1962).

[6] D.G. Eskin, I. Tzanakis, F. Wang, G.S.B. Lebon, T. Subroto, K. Pericleous, J. Mi, Fundamental studies of ultrasonic melt processing. Ultrasonics Sonochemistry **52**, 455-467 (2019). DOI: https://doi.org/10.1016/j.ultsonch.2018.12.028

[7] L.S. García-Colín, S.M.T. De La Selva, The Stokes-Kirchhoff relation in chemically reacting fluids. Chemical Physics Letters **23** (4), 611-613 (1973). DOI: https://doi.org/10.1016/0009-2614(73)89041-4

[8] H. Shekaari, B. Golmohammadi, Ultrasound-assisted of alkali chloride separation using bulk ionic liquid membrane. Ultrasonics Sonochemistry **74**, 105549 (2021). DOI: https://doi.org/10.1016/j.ultsonch.2021.105549

[9] Y. Liu, W. Yu, Y. Liu, Effect of ultrasound on dissolution of Al in Sn. Ultrasonics Sonochemistry **50**, 67-73 (2019). DOI: https://doi.org/10.1016/j.ultsonch.2018.08.029

[10] Y.Zheng, X.Yi Tan, Xiaojuan Wan, X.Cheng, Zh. Liu, Q.Yan, Thermal stability and mechanical response of Bi_2Te_3 – based materials for thermoelectric applications. ACS Applied Energy Materials **3** (3), 2078-2089 (2020). DOI: https://doi.org/10.1021/acsaem.9b02093

[11] A.Chiba, Y.Ohmasa, M.Yao, Vibrational, single-particle-like, and diffusive dynamics in liquid Se, Te, and $Te_{50}Se_50$. J. Chem. Phys. **119**, 9047-9062 (2003). DOI: https://doi.org/10.1063/1.1615234

[12] M. Inui, Y. Kajihara, Y. Tsuchiya, Peculiar temperature dependence of dynamical sound speed in liquid $Se_{50}Te_{50}$ by inelastic x-ray scattering. Journal of Physics Condensed Matter. **21**, 214003 (2020). DOI: https://doi.org/10.1088/1361-648X/ab6d8e

[13] F. Shleifer, J.D. Wilson, R. Loring, Self-consistent theory of polymer dynamic in melts. J. Chem. Phys. **95**, 8474-8485 (1991).

[14] J.M. Liu, W.H. Wu, W. Zhai, B. Wei, Ultrasonic modulation of phase separation and corrosion resistance for ternary *Cu-Sn-Bi* immiscible alloy. Ultrasonics Sonochemistry **54**, 281-289 (2019). DOI: https://doi.org/10.1016/j.ultsonch.2019.01.029

[15] P. Popel, S. Stankus, A. Mozgovoy, R. Khairulin, M. Pokrasin, D. Yagodin, N. Konstantinova, A. Borisenko, M. Guzachev, Physical properties of heavy liquid-metal coolants in a wide temperature range. Conference on liquid and amorphous metals (LAM XVI), Rome, Italy. 104 (2010). DOI: https://doi.org/10.1051/epjconf/20111501014

[16] B.B. Kuliev, P.G. Rustamov, M.A. Aliyanov, E.M. Kuliev, Ultrasonic studies on the interaction of *SnTe-InTe* systems. Physica Status Solidi (a). **4** (2), K127-K130 (1971). DOI: https://doi.org/10.1002/pssa.2210040241

[17] M. Inui, Y. Kajihara, Sh. Hosokawa, K. Matsuda, Y. Tsuchiya, Dynamical sound speed and structural inhomogeneity in liquid *Te* studied by inelastic x-ray scattering. Journal of Non-Crystalline Solids. 1 (2019). DOI: https://doi.org/10.1016/j.nocx.2018.100006